Research article

Lasse Klingbeil*, Christian Eling, Florian Zimmermann, and Heiner Kuhlmann

Magnetic Field Sensor Calibration for Attitude Determination

Abstract: The presented work aims to give an overview of different calibration methods for magnetic field sensors, which are used for attitude determination. These methods are applicable in the field without any additional equipment. However, sometimes they require simplification assumptions. The paper addresses the validity of these assumptions, the accuracy and efficiency of the methods and the influence of the calibration error on the orientation estimation. Both simulations and measurements are used for evaluation. The measurements are performed using a GNSS multi-antenna system, providing an orientation reference (roll, pitch, yaw) without unknown external magnetic disturbances and with a sufficient accuracy (about 0.5 degrees). It is shown in simulations, that a full calibration of the sensor (including soft and hard iron disturbances by nearby materials) is possible without any additional equipment. However, experiments show, that some parts of the full calibration procedure are sensitive to an accurate execution of the necessary movements, which may lead to calibration errors in the same order of magnitude as a simplified method, which ignores the presence of soft iron disturbances.

Keywords: Magnetometer, Calibration, Magnetic Disturbance, Compass, Orientation Estimation, Attitude Determination

DOI: 10.1515/jag-2014-0003
received: January 15, 2014; accepted: April 14, 2014

1 Introduction

Magnetic field sensors, when used as a compass, measure two or three spatial components of the earth magnetic field and therefor enable the determination of the orientation of the sensor unit relative to the magnetic north pole. They are often combined with an inertial measurement unit (accelerometers and angular rate sensors) in order to determine the absolute orientation (regarding 'north' and 'down') of mobile objects. There are not many possibilities to determined the north direction, one is the usage of a gyroscope, which measures the angular rate vector of the earth rotation. However, this is only possible with very expensive and heavy high accuracy gyroscopes and it is only possible when the sensor unit is static. Another possibility is the combination of GNSS observations and inertial sensor data. Here, the translational acceleration component, measured with the inertial sensor unit is compared with the derivatives of the velocity vectors, measured with the GNSS receiver. Obviously, this requires an accelerated motion. A third method is the usage of multiple GNSS antennas, which is described later, as this option serves as an orientation reference within the work for this article. Especially in the field of indoor navigation, magnetic field sensors are very popular, since there are usually no GNSS observations available and therefore magnetic field sensors are the only available north reference.

The main problem with magnetic field sensors is, that they are very sensitive to local disturbances of the earth magnetic field, which may be induced by ferromagnetic material in the vicinity of the sensor. As described later, this material may be part of the environment, leading to disturbances which can not be compensated by calibration, or it is part of the sensor platform, where the magnetometers are attached to. In the latter case, a calibration procedure is in theory capable of finding parameters, that allow to reconstruct the earth magnetic field vector at the position of the sensor.

This contribution does not aim to present a new calibration method for magnetic field sensors, it summarizes the general problem of magnetometer calibration, as already described before in various papers ([18, 23, 4, 11, 7, 2]). It shows, that a calibration, which corrects all sensor errors and disturbing effects of the in-frame sensor environment, can be broken down into an ellipsoid fit and an additional alignment step. The alignment step is necessary, if no external reference data of the magnetic field or the rotation of the sensor is available during calibration. It also presents a method to estimate the alignment matrix, as already described in [10] and [23]. The contribution also does not aim to analyze various ellipsoid fitting methods, as it is done in some of the literature mentioned

***Corresponding Author: Lasse Klingbeil:** Institute of Geodesy and Geoinformation, University of Bonn, Germany, E-mail: klingbeil@igg.uni-bonn.de
Christian Eling, Florian Zimmermann, Heiner Kuhlmann: Institute of Geodesy and Geoinformation, University of Bonn, Germany

above. It uses a Gauss-Helmert model based ellipsoid fitting method, shows its functionality in a simulation, and also presents and discusses an experimental validation of the methods using a GNSS multi-antenna system as an orientation reference.

It should be mentioned here, that the presented methods are also applicable to the calibration of accelerometer triads, since the principle of observing a globally constant vector (earth gravity in this case, the earth magnetic field in the magnetometer case) in the local sensor frame is the same. However, special precautions have to be taken, to make sure that no motion induced translational acceleration components are superimposing the gravity measurement.

2 Sensor Model

The output of a triaxial earth magnetic field sensor is influenced by the following components:

- The actual vector of the earth magnetic field in the sensor frame, which is the variable of interest.
- Properties and imperfections of the sensing element, of the read out electronics and of the mechanical assembly.
- The influence of ferromagnetic materials in the vicinity of the sensor, leading to the addition of permanent magnetic field components ('hard iron effects') or the distortion of the earth magnetic field ('soft iron effects').

The influence of ferromagnetic materials can be further subdivided into effects coming from materials with a constant position in the sensor frame and effects from an interaction with objects in the environment, such as walls, furniture or vehicles. The latter is usually not part of the calibration procedure since these effects are in general location and time variant. Especially in indoor environments, these external disturbance sources are very prominent and have a strong influence on the orientation estimation. Several researchers try to address this issue, for example by estimating the changing disturbance component within a state estimation filter [19]. There are also approaches to utilize the characteristic disturbances of certain objects as landmarks in a localization algorithm (e.g. [8, 12]). We will not consider these effects within this work by minimizing them in the experimental setup. In the following we formulate the various effects mathematically in order to form a basis for any calibration algorithm.

2.1 The earth Magnetic Field

The earth magnetic field is approximately a dipole field (Figure 1, left) with an angle of 11 degrees relative to the rotational axis of the earth. In the context of navigation the field is constant over time, but the field vector $\mathbf{h}_E$ varies over the location on earth. In Germany, where the measurements in this paper have been performed, the length of the vector is 0.487 Gauss and the angle α between the gravitation and the vector is 24 degrees.

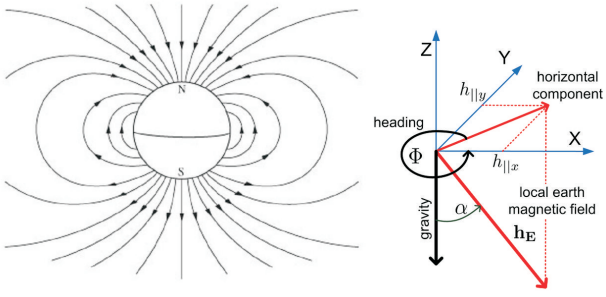

Fig. 1. Left: Magnetic dipole field of the earth; Right: Using the horizontal component of the earth magnetic field to calculate the heading angle. The coordinate system is the sensor frame, assumed to be leveled perpendicular to gravity.

In order to calculate the heading angle ϕ, the horizontal component of the magnetic field vector has to be used (Figure 1, right):

$$\phi = \arctan\left(\frac{h_{||y}}{h_{||x}}\right) \tag{1}$$

If the sensor is not leveled according to the local tangential plane of the earth surface, which is the usual case for mobile sensor systems, the roll and pitch values of the system have to be known from other sensors, such as inclinometers, to determine the horizontal components of the magnetic field vector. In many sensor systems, using a combination of inertial and magnetic sensors to estimate the orientation, the full 3D magnetic field measurement is used as an observation within some sort of Kalman filtering algorithm (see e.g. [20]). In this case a direct determination of the horizontal component is not necessary. Although we use the calibrated magnetometer exactly for this type of application, we refrained from using the Kalman filtered full orientation output for evaluation of the calibration methods, since there are many other parameters influencing the quality of the orientation estimation and the influence of the magnetometer calibration can

not be clearly seen anymore. therefore, we assume the roll and pitch values to be known and compare only heading values directly calculated from (1).

2.2 Triaxial Sensor Model

In an ideal sensor the relation between the applied physical quantity h_{in} and the sensor output h_{out} is given by a linear function $h_{out} = s_s h_{in} + b_s + \epsilon$, where s_s is the scale-factor, b_s the bias (offset) and ϵ the noise of the sensor. In the non-ideal or real sensor the scale factor and bias values are in general time and temperature dependent. We assume these values to be constant, because a one-time calibration would not be possible otherwise. If necessary, the varying parameters have to be continuously estimated in some sort of in-run estimation, where the parameters derived by the presented method can be used as an initial value. In principle the scale factor depends on the applied physical quantity itself, leading to sensor non-nonlinearities, or even on the history of these quantities, leading to hysteresis effects. According to the literature (e.g.[2]) We assume these effects to vanish as well. Another non-ideality is sensor noise originated in the sensing element or the read out electronics. We assume the noise here to be normally distributed and white (more details on the noise characteristic can be found in [18]).

In a triaxial sensor setup three orthogonal single axis sensors are combined in a single sensor unit, leading to a scale-factor matrix $S_s = \mathrm{diag}(s_{s1} \quad s_{s2} \quad s_{s3})$ and a bias vector $\mathbf{b}_s = [b_{s1} \quad b_{s2} \quad b_{s3}]^T$. In general there may be a misalignment of the three axis and also of the whole triplet within the sensor frame, which can be modeled by the Matrix $C_{ma} = [\mathbf{n}_1 \quad \mathbf{n}_2 \quad \mathbf{n}_3]^{-1}$, where $\mathbf{n}_i$ are the directions of the sensor axis within the sensor frame. There may also be a sensor specific cross coupling between the different sensor axis, which can be modeled as a matrix C_{cc}, which is symmetrical in most cases. For example in single-die MEMS accelerometers, where all three mechanical sensor elements are implemented on a single silicon chip, this can lead to cross axis sensitivities up to 5% [24].

In total the sensor model can be written as

$$\mathbf{h}_{out} = S_s C_{cc} C_{ma} \mathbf{h}_{in} + \mathbf{b}_s + \epsilon, \tag{2}$$

where ϵ is Gaussian wide-band noise. It is more convenient to define a combined 'scale-factor matrix' $C_s = S_s C_{cc} C_{ma}$, since the specific effects are usually not re-constructable from any calibration procedure. In a simplified sensor model, with orthogonal axis and without cross-axis sensitivity C_s reduces to the diagonal matrix S_s.

2.3 Disturbance Model

The sensor is exposed to the physical quantity $\mathbf{h}_{in}$. In an ideal sensor environment $\mathbf{h}_{in}$ is the earth magnetic field $\mathbf{h}_E^N$, measured in the coordinate frame of the sensor:

$$\mathbf{h}_{in} = \mathbf{h}_E^S = R_N^S \mathbf{h}_E^N. \tag{3}$$

The upper index indicates the coordinate system in which the vector is expressed ('N' for navigation frame, 'S' for body frame) and R_N^S is the rotation from the navigation frame to the sensor frame. However, ferromagnetic materials in the vicinity of the sensor may disturb the quantity of interest, that is the earth magnetic field, in two ways, known as 'hard iron' and 'soft iron' effects. Without going into to details here (see [3]), those effects can be described as follows.

Hard iron effects come from permanent magnets in the sensor environment and simply add an additional component to earth magnetic field. Assuming, that all disturbing material is fixed within the sensor frame, the hard iron effect leads to a constant offset $\mathbf{b}_{hi}$ for all sensor readings.

Soft iron effects come from a more complex interaction of the present earth magnetic field with ferromagnetic material close to the sensor. This interaction leads to a distortion (bending, scaling) of the external field depending on the relative orientation between the external field and the material. The soft iron effect can be modeled as a general matrix C_{si} disturbing the earth magnetic field in the sensor frame. Here a linear model is assumed, neglecting non-linear and hysteresis effects [22].

Combining hard and soft iron effects, the sensor is exposed to the field

$$\mathbf{h}_{in} = C_{si} R_N^S \mathbf{h}_E^N + \mathbf{b}_{hi}. \tag{4}$$

With (2) and (4) the complete sensor model including sensor errors and magnetic disturbances becomes

$$\mathbf{h}_{out} = C\mathbf{h}_E^S + \mathbf{b} + \epsilon, \tag{5}$$

where

$$C = S_s C_{cc} C_{ma} C_{si}, \tag{6}$$

$$\mathbf{b} = S_s C_{cc} C_{ma} \mathbf{b}_{hi} + \mathbf{b}_s. \tag{7}$$

Another disturbing effect one has to be aware, when operating sensor systems with magnetic field sensors, is the magnetic fields induced by current-carrying cables and conductors. If these cables are located on fix positions within the sensor frame and the current is constant

over time, they have the same effect as a hard iron disturbance, adding a constant magnetic field component to the measurement. However, currents are often time varying in electronic systems and these effects should be minimized by the mechanical setup and the placement of the components. We do not consider this within the presented work.

3 Calibration Algorithm

3.1 Problem Formulation

The goal of the calibration procedure is to determine C and $\mathbf{b}$ for a specific sensor setup, in order to reconstruct the undisturbed earth magnetic field in the sensor frame from the sensor readings:

$$\mathbf{h}_E^S = C^{-1}(\mathbf{h}_{out} - \mathbf{b}). \tag{8}$$

If it would be possible to measure a large number of sensor readings $\mathbf{h}_{out}$ for known earth magnetic field vectors $\mathbf{h}_E^S$ in the sensor frame, the matrix C and the offset $\mathbf{b}$ could be determined directly using some sort of parameter estimation algorithm. The problem in an field calibration is, that usually the input magnetic field $\mathbf{h}_E^S = R_N^S \mathbf{h}_E^N$, which can be calculated from the known earth magnetic field vector $\mathbf{h}_E^N$ and the known rotation R_N^S of the sensor with regards to the earth frame, is not known. However, we know that if we would rotate an ideal sensor arbitrarily in an undisturbed environment, all magnetic field measurements in the sensor frame would lie on the surface of a sphere around the point of origin, since the earth magnetic field can be assumed to be homogeneous on the local scale. As explained in the following, the matrix C and the offset $\mathbf{b}$, which come from all sensor imperfections and external disturbances transform this sphere into a rotated and shifted ellipsoid (see Figure 2).

From standard linear algebra we know, that every matrix can be expressed as a multiplication of three special matrices (SVD - Singular Value Decomposition, e.g. [17]):

$$C = UDV^T, \tag{9}$$

where $U, V \in O(3)$ and D is diagonal. Therefore equation (5) can be written as

$$\mathbf{h}_{out} = UDV^T \mathbf{h}_E^S + \mathbf{b} + \epsilon. \tag{10}$$

Using this notion it can be seen, that if all points $\mathbf{h}_E^S$ lie on the surface of a sphere, all points $\mathbf{h}_{out}$ will be on the surface of an ellipsoid, which half axis are given by the diagonal elements of D ('stretching' of the sphere), which is rotated by the rotation matrix U and which is translated by the vector $\mathbf{b}$ relative to the origin of the frame (Figure 2). Therefore, a major part of the magnetometer calibration process can be seen as an ellipsoid regression problem, where the half-axis, the offset vector and three rotation angles are estimated. However, it is very important to note, that the matrix V^T, which corresponds to a rotation of the sphere, before scaling, rotating and shifting it to the form of the ellipsoid, is not a parameter which can be estimated by the ellipsoid regression. This is because only the geometry of the points cloud is determined and the point to point correspondence is lost, which is needed for a proper reconstruction of the magnetic field values from the sensor readings. This rotation, according to [22] we call it 'alignment matrix', has to be determined using an additional calibration step.

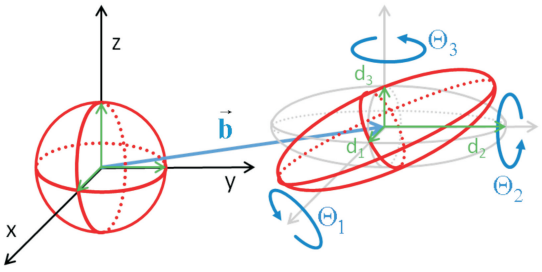

Fig. 2. Transformation of a sphere to an ellipsoid. The half axis d_1, d_2, d_3 correspond to the matrix D, the rotation angles Φ_1, Φ_2, Φ_3 correspond to the matrix U, and $\mathbf{b}$ is the offset. The matrix V^T is a rotation of the sphere and does not change the geometry of the the ellipsoid.

3.2 Calibration Procedure

The complete calibration procedure comprises the following steps:

Acquiring data

A set of sensor data is recorded while the whole sensor setup including the system, where it is mounted, is rotated in a way, that the rotation distribution is spread over the whole sphere as much as possible.

Fitting the ellipsoid

An ellipsoid is fitted to the recorded sensor data in order to estimate D, U as factors of the calibration matrix C and b, which is the combined offset. There are a number of different ellipsoid fitting algorithms in literature (e.g. [21, 14, 6, 16]) and an analysis of all of them is beyond the

scope of this paper. In this work we use a Gauss-Helmert model method, derived from [15]. In this method a Total Least Squares estimation with non linear-constraints is used in order to get a bias free estimate of a non-linear problem with noisy observation. See [13] for estimation using Gauss-Helmert models or [9] for a comparison of Gauss-Helmert and Gauss-Markov models.

Getting the missing rotation

First an initial set $\mathbf{h}'^{S}_{E}$ of local magnetic field values is reconstructed using the estimated ellipsoid parameters U,D and $\mathbf{b}$:

$$\mathbf{h}'^{S}_{E} = D^{-1}U^{-1}(\mathbf{h}_{out} - \mathbf{b}). \tag{11}$$

If the ellipsoid estimation was successful so far, all sensor readings will already be on the surface of an sphere. However, the final rotation V, which is a rotation of that sphere still has to be determined:

$$\mathbf{h}^{S}_{E} = V\mathbf{h}'^{S}_{E} \tag{12}$$

This is only possible, when some sort of reference information are available during the calibration process:

Additional sensors as reference

There are other sensors available, such as accelerometers or gyroscopes, allowing to estimate this rotation within the calibration procedure. We do not consider this method in this work. A nice description can be found in [11].

Absolute orientations as reference

There exists a reference data set, where the rotation R^{S}_{N} is known for every sensor reading. Then the missing rotation V^{T}can be reconstructed by a simple parameter estimation procedure. In our work we use the orientation angles, determined using a GNSS multi-antenna system, as a reference to predict the true magnetometer readings $\mathbf{h}^{S}_{E}$ of the sensors. An ICP (iterative closest point [1]) algorithm is then used to determine the missing rotation V between the 'precalibrated' sensor readings $\mathbf{h}'^{S}_{E}$ and the predicted values $\mathbf{h}^{S}_{E}$ (equation 12).

Relative rotations as reference

There are no absolute reference data and no additional sensors available. In this case the missing rotation can be estimated by measuring sensor data in three different orientations of the sensor frame, where only the relative rotation needs to be known.

In the following the method using the relative rotations is described in more detail, since it offers a way to estimate all calibration parameters without the need for an absolute orientation reference data set. Assuming we measure the reconstructed value $\mathbf{h}'_0$ in an arbitrary initial orientation, we know from (12), that we actually measure

$$\mathbf{h}'_0 = V^{T}\mathbf{h}_0 \tag{13}$$

Rotating the sensor unit with a known rotation R, we measure another value

$$\mathbf{h}'_1 = V^{T}R\mathbf{h}_0 \tag{14}$$

With the rotation T, which rotates $\mathbf{h}'_0$ into $\mathbf{h}'_1$ and (13) we can write

$$T\mathbf{h}'_0 = V^{T}R\mathbf{h}_0 \tag{15}$$

$$= V^{T}RV\mathbf{h}'_0. \tag{16}$$

For two known rotations R_i, $i = 1, 2$ we can write

$$T_i = V^{T}R_iV \tag{17}$$

Since the transformation V is only changing the rotation axis and not the rotation angle of a rotation, we can write

$$T_i = R(V^{T}\mathbf{d}_i, \phi_i). \tag{18}$$

If we determine T_i from the measurement and build the angle axis representation $(\mathbf{d}_{Ti}, \phi_i)$, where the ϕ_i are constraint to be the same angles as for the known rotations R_i, we can estimate V from the transformation of the rotation axis:

$$\mathbf{d}_{Ti} = V^{T}\mathbf{d}_i. \tag{19}$$

In short words, we apply two rotations around known axis $\mathbf{d}_i$, we measure the sensor output and determine the rotation axis $\mathbf{d}_{Ti}$ from the measurement and we estimate the transformation, which rotates the axis $\mathbf{d}_i$ into $\mathbf{d}_{Ti}$.

Figure 3 shows an example, how the three distinct orientations, starting from an arbitrary orientation, followed by two known rotations around the sensor axis, may look like. This sequence was used in the calibration procedure described later.

4 Simulation

In order to demonstrate the functionality of the complete calibration algorithm, a simulation has been performed doing the following steps:

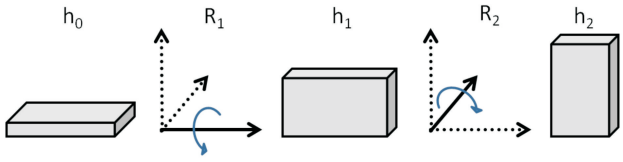

Fig. 3. Example of the three distinct orientations, used for the determination of the alignment matrix within the calibration procedure.

1. Simulation of a reference angular motion trajectory (roll, pitch, yaw)
2. Simulate magnetic field sensor data for each rotation using the following sensor errors and magnetic disturbances (the local earth magnetic field vector length is without loss of generality assumed to be equal to one. All noise values and the calculated residuals relate to this vector length):

Sensor errors

- sensor noise: 0.005 standard deviation for all axis
- sensor offset [x,y,z]: (0.2, 0.1, 0.3)
- axis non-orthogonalities: ± 1 degree for y- and z-axis
- axis cross coupling: 1% of each axis couples to every other axis (assumed to be symmetric)

Disturbance errors

- Hard iron offset [x,y,z]: (0.5, 0.4, 0.2)
- Soft iron matrix $C_{si} = \begin{pmatrix} 0.58 & -0.73 & 0.36 \\ 1.32 & 0.46 & -0.12 \\ -0.26 & 0.44 & 0.53 \end{pmatrix}$

  (taken from the simulation example in [22])
3. Get the ellipsoid parameters U, D, $\mathbf{b}$ from the simulated sensor data set using the Gauss-Helmert model.
4. Get the missing rotation V^T using the simulated reference trajectory and the ICP algorithm as described before.

The top of Figure 4 shows the simulated sensor data and the reconstructed ellipsoid. It can be clearly seen, that the simulated sensor errors and magnetic disturbances indeed lead to a rotated and translated ellipsoid. The reconstructed magnetic field values (green) and the values used as a reference trajectory (red) are shown in the bottom of the figure.

The top of Figure 5 shows the error distribution of the reconstructed magnetic field values for each

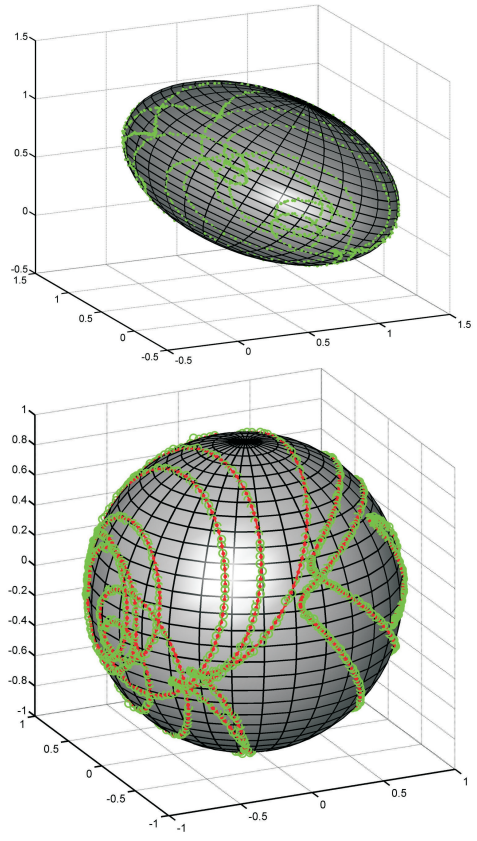

Fig. 4. Top: Simulated sensor data and ellipsoid, which has been fitted to the data. Bottom: Reconstructed Magnetic field values (green) and values of the reference trajectory (red).

sensor axis. The standard deviation of the errors is $(0.004, 0.006, 0.008)$ for the (x, y, z) axis and is therefore in the order of the sensor noise which has been used in the simulation. The error distribution of the reconstructed heading is shown on the bottom left. The standard deviation is 0.9 degree. For the heading computation the roll and pitch of the reference trajectory has been used to project the magnetic field vector reading to the horizontal plane. The bottom middle and right charts of the figure show the distribution of the vector length of the magnetic field reading before and after calibration. This distribution is always a good indicator how well the calibration has performed even in the case of missing reference data. Since the calibration principle is to bring all sensor readings back on the surface of a sphere, we expect a sharp distribution around one.

The simulation shows, that all error and disturbance effects, that have been mentioned in the beginning can be compensated using the calibration procedure described above, with the following assumptions:

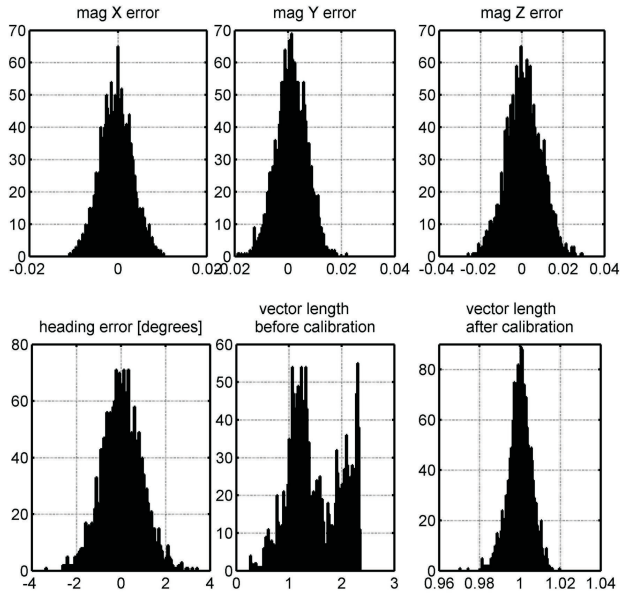

Fig. 5. Top: Error distribution of the reconstructed magnetic field values. Bottom left: reconstructed heading error. Bottom middle and right: vector length of the magnetic sensor readings before and after calibration.

- All errors and disturbances are not time varying.
- The soft iron effects are linear.
- There exists a possibility to reconstruct the missing rotation (alignment matrix). In the simulation we use the reference trajectory to estimate it.

In the next section we show experiments, where we compare the two different methods to determine the missing rotation with a simpler calibration method and with the factory calibration of the sensor.

5 Experimental Evaluation

5.1 Experimental setup

For the experimental evaluation we built a system, which is shown in Figure 6. Three geodetic GNSS receiver antennas are mounted on a rectangular aluminum structure, forming two GNSS baselines $B1$ and $B2$. The baseline length is about 60cm. The carrier phase observations of the receivers are used to calculate the baseline vectors in a global coordinate frame, allowing the reconstruction of the roll, pitch and yaw angles of the setup [5]. These angles are used as an orientation reference in the following experiments. The device under test is a three axis magnetic field

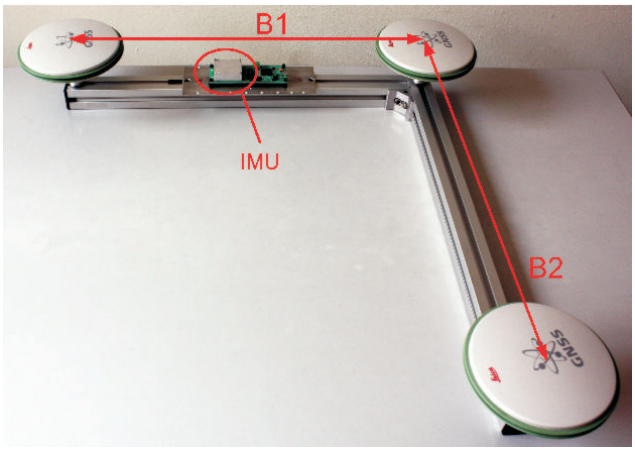

Fig. 6. Orientation reference system based on three geodetic GNSS receivers.

sensor, which is part of an ADIS16488 tactical grade MEMS based Inertial Measurement Unit (IMU), is mounted to one of the aluminum beams. This setup minimizes the amount of ferromagnetic material in the vicinity of the magnetic field sensor, and allows a reconstruction of the orientation with an accuracy of about 0.5 degrees, using the two GNSS baselines. In the experiments these orientation angles are used as a reference to evaluate the performance of the different calibration procedures. In one of the procedures the data are used to determine the missing rotation, as described before. We are also able to attach a block of steel close to the sensor unit, to create a soft iron effect, affecting the magnetic field measurement (Figure 7). Note, that within this paper we do not make any use of the the gyroscope and the accelerometer within the IMU.

We investigated two setups of the sensor system. One setup has the steel block attached close to the sensor unit (**disturbed case**), creating a soft iron effect. In the other one the steel block has been removed (**undisturbed case**) to create a mostly undisturbed environment. For each of the setups we recorded three data sets:

CalDataset
For this data set, the whole system was rotated randomly around all possible axis for about two minutes. Reference angles could not be recorded during these measurements, since the antennas are turned upside down several times.

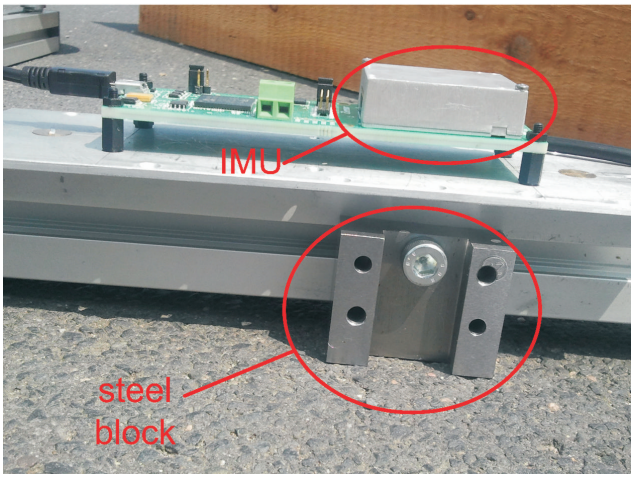

Fig. 7. Block of steel mounted close to the sensor unit, creating a soft iron effect.

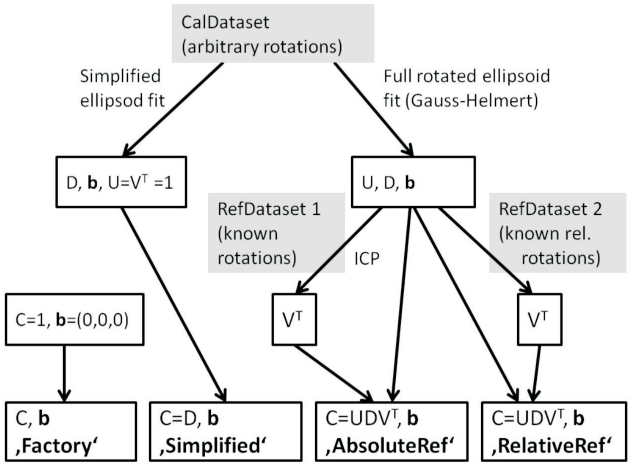

Fig. 8. Scheme of the different calibration methods, which has been compared using the experimental data.

RefDataset 1
For this data set, the system was rotated randomly, but keeping the roll and pitch values below 45 degrees. In parallel, the GNSS observation have been recorded and the roll, pitch and yaw angles have been calculated. With this data the method *AbsoluteRef* can be used for the determination of the missing rotation. It is also used as a reference for the full calibration procedure, since the true heading values of the system are known for each sensor reading.

RefDataset 2
This data set consists of recordings of the magnetic field values in three distinct orientations of the sensor system according to method *RelativeRef*. These orientations are unknown, but the rotation axes and angle between them are known in the sensor frame. Those will be used to reconstruct the alignment matrix as described above.

As shown in Figure 8, we created four different calibration parameter sets (C, $\mathbf{b}$) for both cases, the disturbed and the undisturbed one:

Factory
The factory calibration of the magnetic field sensor is used. Usually the manufacturer provides some sort of default calibration, which quality strongly depends on the price of the sensor unit.

Simplified
In a simple case, where all soft iron effects, axis non-orthogonalities and cross axis couplings vanish, the calibration matrix C reduces to the scale-factor matrix S_s and the ellipsoid is not rotated at all. Clearly in this case the estimation of the second rotation is not needed, as there is also no first rotation U.

AbsoluteRef
A rotated ellipsoid is fitted to the calibration data set using the Gauss-Helmert model. The missing rotation is calculated using an ICP algorithm and the known absolute orientations (RefDataset 1) as described in section 3.2.

RelativeRef
A rotated ellipsoid is fitted to the calibration data set using the Gauss-Helmert model. The missing rotation is estimated from three additional measurements with known relative orientations (RefDataset 2) as described in section 3.2.

5.2 The undisturbed case

The ellipsoid fit has been applied to the calibration data set in the undisturbed case. In Table 1 the parameters of the reconstructed rotated ellipsoid (using the Gauss-Helmert model) and the ones from the estimation of a non-rotated ellipsoid (simplified fit) are compared with the factory cal-

ibration. All axis of the factory calibrated sensor data have been scaled with 0.4870, which is the theoretical value to scale the data (given in mGauss) to units, where the earth magnetic field vector length would be one. Note, that the

Table 1. Reconstructed ellipsoid parameters in the undisturbed case.

	Factory	Gauss-Helmert	Simplified
	0.4870	0.4798	0.4800
half axis	0.4870	0.4776	0.4810
	0.4870	0.4825	0.4782
	0	0.0035	0.0038
offset	0	-0.0002	-0.0005
	0	-0.0165	-0.0164

axis directions of the ellipsoid, which is fitted with the Gauss-Helmert model, are not in the sensor frame, since the missing rotation is not yet applied at that point. Therefore the individual axis parameters can not be compared here. From the Table 1 it can be seen, that the estimated half axis are very similar for all axis and also for all fitting methods. It is obvious, that fitting a rotated ellipsoid to a noisy data set, which represents nearly a sphere can be very problematic, since the three rotation parameters are not observable anymore.

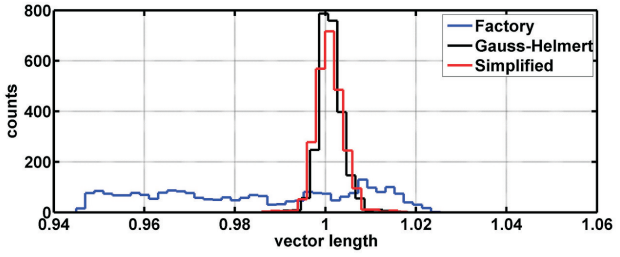

Fig. 9. Vector length distribution of the reconstructed magnetic field values in the undisturbed case.

Figure 9 shows the distribution of the vector length of the reconstructed magnetic field values in the calibration data set. After fitting the ellipsoid, this is a good indicator, if the fit was successful. In the ideal case, all values have the same length. The factory calibrated length values are spread over a range of about 6% of the earth magnetic field, while the other two fitting methods bring the length into a range of about 0.5%.

After the ellipsoid fitting, the missing rotation V^T has been reconstructed using the methods described above. This was only necessary for the Gauss-Helmert ellipsoid, since this one is rotated. After this step the complete calibration matrix $C = UDV^T$ is known, and the calibration has been evaluated using the reference data set 'Ref-Dataset 1'. Figure 10 shows the roll, pitch and heading angles during the motion. For evaluation, the heading angles have been calculated from the reconstructed magnetic field values. To do this, the magnetic field vectors had to be projected into the horizontal plane. For this projection, the roll and pitch values have to be known, in this case the reference values were taken. Figure 11 shows the distribution of the heading errors for the different calibration methods. The errors show a very similar distribution, which is not surprising, since in an undisturbed case even the factory calibration should also lead to acceptable results. The soft iron disturbances, which (together with the cross-axis coupling and axis non-orthogonalities) effectively lead to a rotated ellipsoid are very small in this case. Ignoring these effects, as it is done when fitting a non-rotated ellipsoid, leads to similar results as with the full parameter set. As we will see later, a stronger soft iron effect will lead to larger differences between the calibration methods.

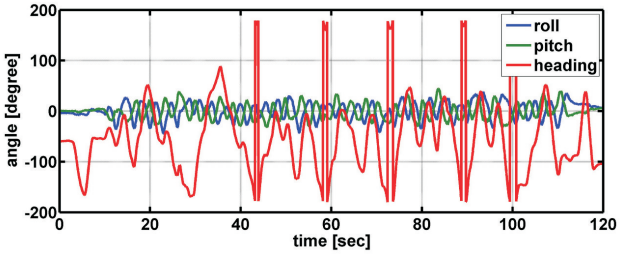

Fig. 10. Reference orientations of the undisturbed case calculated with the data from the GPS antennas.

However, the heading residuals for the 'RelativeRef' case show a small offset of about one degrees. This is very likely to come from the reconstruction of the missing rotation using the three distinct orientations. The relative orientation between them has to be known exactly, but in practice this is difficult to realize. In our experiments we used the lid of a wooden box, trying to realize 90 degrees turns, but they could have been easily a few degrees off. One can conclude, that in an undisturbed or slightly disturbed case all methods show similar results and therefore

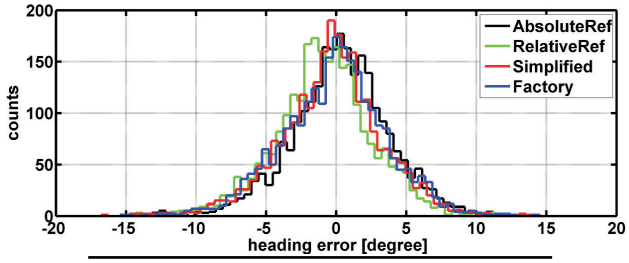

	Abs.Ref	Rel.Ref	Simpl.	Factory
mean	0.0810	-1.1289	-0.5699	-0.4186
std	3.5212	3.5892	3.6829	3.7272

Fig. 11. Distribution of the heading reconstruction errors in the undisturbed case for all calibration methods.

the simplest one, which is the fitting of an non-rotated ellipsoid should be used.

5.3 The disturbed case

For the disturbed case with the steel block attached close to the magnetic field sensor the same analysis has been performed. Table 2 shows the solutions of the ellipsoid fitting procedures.

Table 2. Reconstructed ellipsoid parameters in the disturbed case.

	Factory	Gauss-Helmert	noRotation
	0.4870	0.4600	0.4402
half axis	0.4870	0.5355	0.4770
	0.4870	0.4439	0.5143
	0	-0.0252	-0.0172
offset	0	-0.0094	-0.0236
	0	-0.0041	-0.0066

Figure 12 shows the calibration data set and the rotated ellipsoid, which has been fitted using the Gauss-Helmert model.

It can be clearly seen, that in this case the half axis are not the same and that the estimated ellipsoid is rotated. In Figure 13 the distributions of the length of the reconstructed magnetic field vectors are shown. The Gauss-Helmert ellipsoid shows a significant improvement compared to the factory calibration and the estimation of an unrotated ellipsoid.

The roll, pitch and heading angles of the reference data set are shown in Figure 14.

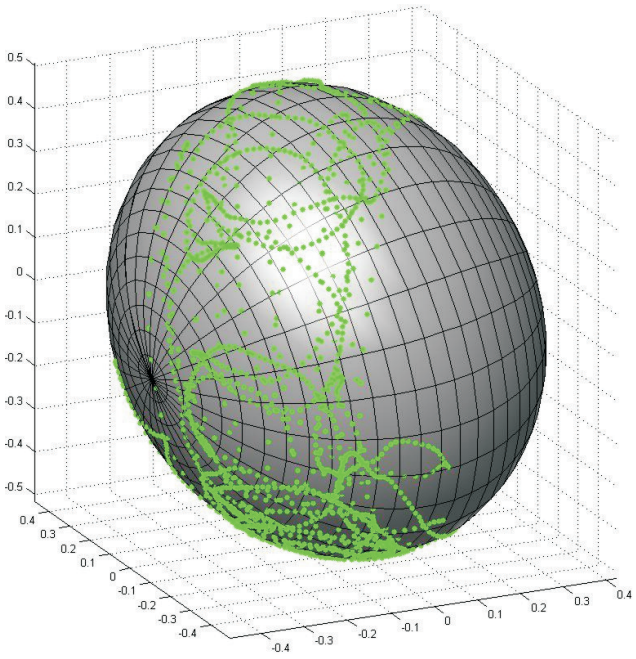

Fig. 12. Calibration data set and fitted rotated ellipsoid for the disturbed case.

The error distributions of the reconstructed heading angles for all calibration methods are shown in Figure 15.

As expected, the method which uses the rotated ellipsoid fitting and gets the missing rotation from a reference data set shows the best performance. Also expected, the factory calibrated data lead to large errors in the heading reconstruction. The errors resulting from the calibration using the three additional measurements (*RelativeRef*) have a similar distribution as the ones from the *AbsoluteRef* method, but again there is an offset of about three degrees, which can be explained as before. A somewhat surprising result is the performance of the *Simplified* method, where only the scale factors for each axis and

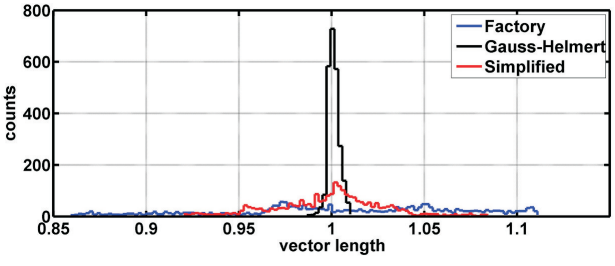

Fig. 13. Vector length distribution of the reconstructed magnetic field values in the disturbed case.

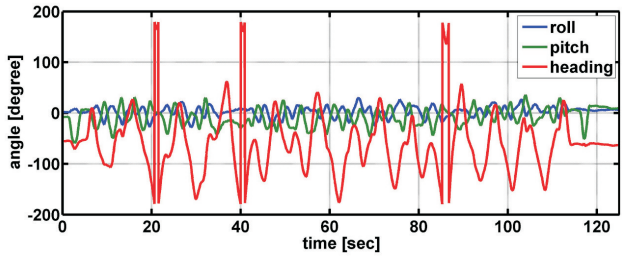

Fig. 14. Reference orientations of the disturbed case, calculated with the data from the GPS antennas.

the offsets are estimated. It shows a very similar performance as the *RelativeRef* calibration. Apparently, the errors which can be induced by the missing rotation reconstruction procedure are in the same order as the ones, ignoring the soft iron effects and other 'ellipsoid rotating' effects completely. Of course, this would not be the case for a rotated ellipsoid with bigger differences in the length of the half axis.

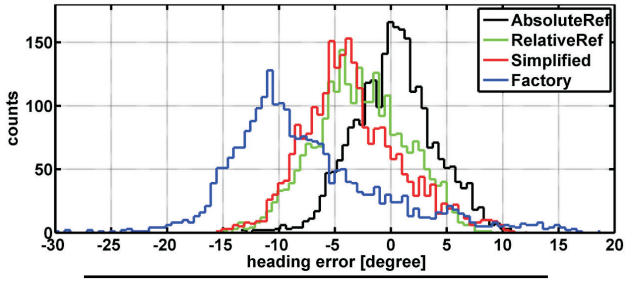

	Abs.Ref	Rel.Ref	Simpl.	Factory
mean	0.0517	-2.9476	-3.6522	-7.7819
std	3.6227	4.0932	4.3959	6.9666

Fig. 15. Distribution of the heading reconstruction errors in the disturbed case for all calibration methods.

6 Conclusion

In this work the general problem of magnetometer calibration has been recapitulated. It was shown, that if all linear sensor and environmental disturbance errors are considered, the calibration procedure corresponds to the task of estimating 12 parameters of a linear transformation, consisting of a general 3x3 Matrix and an offset vector. The input values to this transformation are the earth magnetic field vector in the local sensor frame, which form the surface of a sphere, since the length is constant. The output values of this transformation lie on the surface of a rotated ellipsoid, whose nine parameters can be estimated using various methods. However, three parameters are still unknown, since they correspond to a rotation of the sphere, before it is scaled and rotated to the form of the ellipsoid. Two methods have been presented, how this extra parameters can be estimated using different types of reference data. One method needs the absolute orientation of the sensor systems, which have to be determined by other methods, such as a GNSS multi-antenna system. The other method does not need any external reference system, but an additional calibration step is necessary. It is based on the measurement of a set of distinct orientations, which absolute values are unknown, but which have a known relation to each other in the sensor frame. Using experimental data, it has been shown, that this method is in principle successful.

However, the experiments show, that this procedure is sensitive to errors, because a known rotation has to be applied to the sensor frame (such as 'rotating it 90 degrees around its x-axis'), which may be difficult, depending on the size and the casing of the sensor unit. In the experiment, the calibration procedure using this reference free method of getting the alignment matrix shows a similar performance as the calibration, where any off-diagonal elements of the calibration matrix (soft iron effects, axis non-orthogonalities, cross-axis coupling) are ignored, which corresponds to the fitting of a non rotated ellipsoid to the data. Since the disturbance, which was created by attaching a steel block close to sensor unit is a rather strong one, it can be concluded, that for moderate disturbances, the simple calibration procedure is sufficient. In the case of strong soft iron disturbances, and when the application of additional rotations as in the *RelativeRef* method are not feasible, the only chance to get the full calibration parameter set is by acquiring reference data or using additional sensors, which may be available in the system (e.g. as described in [11]).

Based on our experiences and the results presented in this work, we want to conclude with the following statements:

- Even for higher grade magnetic field sensors, which usually provide factory calibration parameters, a calibration of the sensor within the full operating sensor system is necessary, since the calibration parameters depend on the properties of the environment close to the sensor.
- Minimizing the effects of soft and hard iron and of electrical currents should be done within the design phase of the system, by placement of the system and the choice of the used materials.

- For an accurate calibration in the presence of strong soft iron effects reference data are necessary during the calibration. These reference data do not have to be necessarily absolute orientation information, relative rotation information are sufficient.
- In the case of moderate or no soft iron effects and an accurate axis orthogonality a simplified calibration procedure without the need for any reference data is sufficient.
- In the ideal case in our experiment, where an absolute reference data was available, the reconstructed heading values after calibration had an accuracy of about 3.5 degrees. Of course this result depends on the sensor noise, the quality of the reference data and the accuracy of the roll and pitch data, needed for the heading calculation. The accuracy also depends on the location of the measurement, since the signal-to-noise ratio of the horizontal magnetic field component is higher in regions where the magnetic inclination angle is smaller, as it is for example in the equator regions.

Acknowledgments

The authors gratefully acknowledge funding of parts of this work by the German Research Foundation (DFG), within the research group FOR 1505 'Mapping on Demand'.

References

[1] Chen Y. and Medioni G., Object modeling by registration of multiple range images, in: Robotics and Automation, 1991, Proceedings, IEEE International Conference on 3 (1991), 2724–2729.

[2] Crassidis J. L., Lai K.-L. and Harman R. R., Real-time attitude-independent three-axis magnetometer calibration, *Journal of Guidance, Control, and Dynamics* 28 (2005), 115–120.

[3] Denne W., *Magnetic Compass Deviation and Correction*, Sheridan House Inc, (1979).

[4] Dorveaux E., David Vissiére D., Martin A.-P. and Petit N., Iterative calibration method for inertial and magnetic sensors, in: *Decision and Control, 2009 held jointly with the 2009 28th Chinese Control Conference. CDC/CCC 2009, Proceedings of the 48th IEEE Conference on*, IEEE, 8296–8303, 2009.

[5] Eling C., Zeimetz P. and Kuhlmann H., Development of an instantaneous GNSS/MEMS attitude determination system, *GPS solutions* 17 (2013), 129–138.

[6] Fitzgibbon A., Pilu M. and Fisher R. B., Direct least square fitting of ellipses, *Pattern Analysis and Machine Intelligence, IEEE Transactions on* 21 (1999), 476–480.

[7] Gebre-Egziabher D., Elkaim G. H., Powell J. D. and Parkinson B. W., A non-linear, two-step estimation algorithm for calibrating solid-state strapdown magnetometers, in: *Proceedings of the International Conference on Integrated Navigation Systems*, 28–30, 2001.

[8] Gozick B., Kalyan Subbu K. P., Dantu R. and Maeshiro T., Magnetic maps for indoor navigation, Instrumentation and Measurement, *IEEE Transactions on* 60 (2011), 3883–3891.

[9] Kanatani K. and Hirotaka Niitsuma H., Optimal computation of 3-D similarity: Gauss–Newton vs. Gauss–Helmert, *Computational Statistics Data Analysis* 56 (2012), 4470–4483.

[10] Klingbeil L., *Entwicklung eines modularen und skalierbaren Sensorsystems zur Erfassung von Position und Orientierung bewegter Objekte*, Ph.D. thesis, Universitaet Bonn, Physikalisches Institut, 2006.

[11] Kok M., Hol J. D., Schon T. B., Gustafsson F. and Luinge H., Calibration of a magnetometer in combination with inertial sensors, in: *Information Fusion (FUSION), 15th International Conference on*, IEEE, 787–793, 2012.

[12] Le Grand E. and Thrun S., 3-Axis magnetic field mapping and fusion for indoor localization, in: *Multisensor Fusion and Integration for Intelligent Systems (MFI), IEEE Conference on*, 358–364, 2012.

[13] Lenzmann L. and E Lenzmann E., Strenge Auswertung des nichtlinearen Gauß-Helmert-Modells, *Allgemeine Vermessungs-Nachrichten* 2 (2004), 68–73.

[14] Li Q. and Griffiths J. G., Least squares ellipsoid specific fitting, in: *Geometric Modeling and Processing, 2004. Proceedings*, IEEE, 335–340, 2004.

[15] Nitschke M., Loesler M., Bestimmung der Parameter einer Regressionsellipse in allgemeiner Raumlage, *Allgemeine Vermessungs-Nachrichten* 3 (2010), 113–117.

[16] Markovsky I., Kukush A. and Van Huffel S., Consistent least squares fitting of ellipsoids, *Numerische Mathematik* 8 (2004), 177–194.

[17] Press W. H., *Numerical recipes 3rd edition: The art of scientific computing*, Cambridge university press, 2007.

[18] Renaudin V., Afzal M. H. and Lachapelle G., Complete Triaxis Magnetometer Calibration in the Magnetic Domain, *Journal of Sensors* 2010 (2010), 1–10.

[19] Roetenberg D., Luinge H. J., Baten C. T. M and Veltink P. H., Compensation of magnetic disturbances improves inertial and magnetic sensing of human body segment orientation, *Neural Systems and Rehabilitation Engineering, IEE Transactions on* 13 (2005), 395–405.

[20] Romanovas M., Klingbeil L., Traechtler M. and Manoli Y., Efficient Orientation Estimation Algorithm for Low Cost Inertial and Magnetic Sensor Systems, in: *2009 IEEE Workshop on Statistical Signal Processing, IEEE*, Cardiff, Wales, UK, 2009.

[21] Turner D. A., Anderson I. J., Mason J. C. and Cox M. G., An algorithm for fitting an ellipsoid to data, *National Physical Laboratory*, UK, 1999.

[22] Vasconcelos F., Elkaim G., Silvestre C., Oliveira P. and Cardeira B., A geometric approach to strapdown magnetometer calibration in sensor frame, *Navigation, Guidance and Control of Underwater Vehicles* 2 (2008), 1–11.

[23] Vasconcelos J. F., Elkaim G., Silvestre C., Oliveira P. and Cardeira B., Geometric approach to strapdown magnetometer calibration in sensor frame, *Aerospace and Electronic Systems, IEEE Transactions on* 47 (2011), 1293–1306.

[24] Weston J. L. and Titterton D. H., Modern inertial navigation technology and its application, *Electronics Communication Engineering Journal* 12 (2000), 49–64.